

FIG. 1. Experimental setup (dimensions in mm).

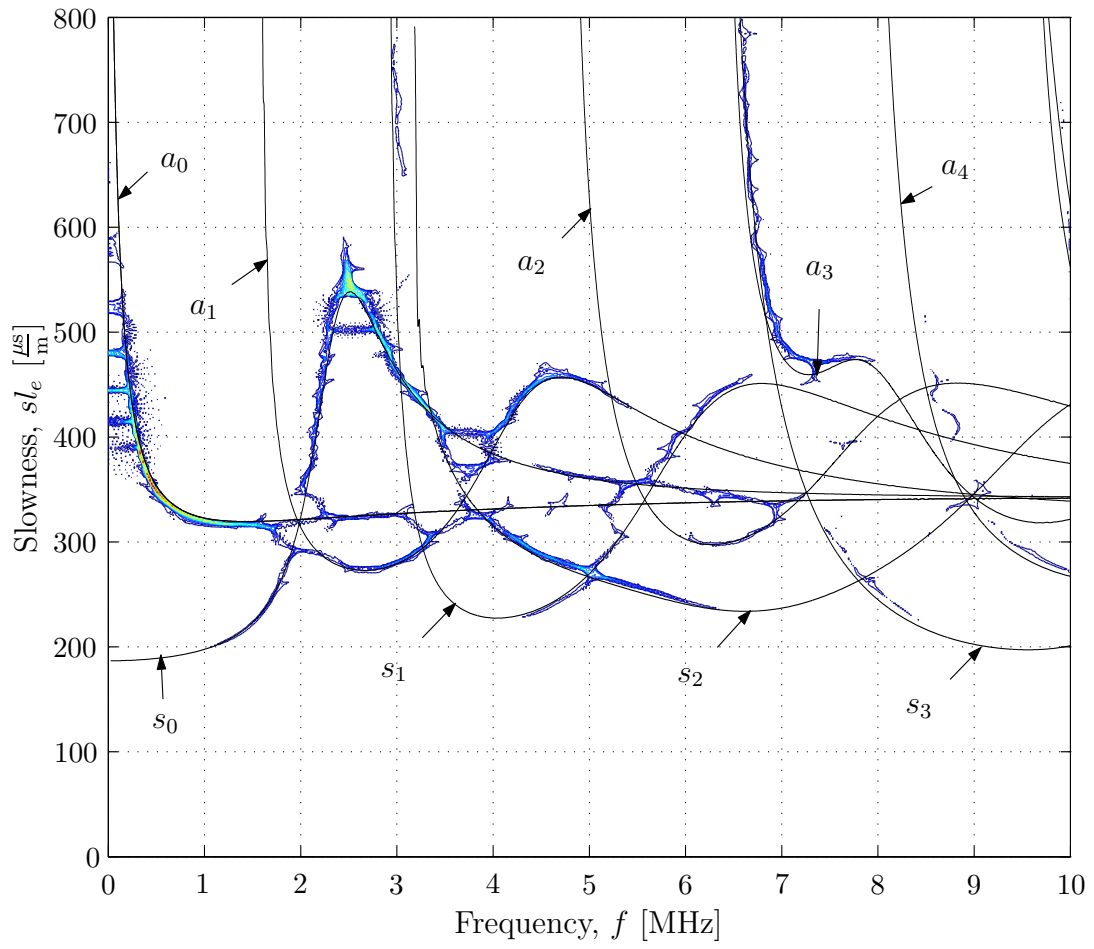


FIG. 2. SFR of perfect plate.

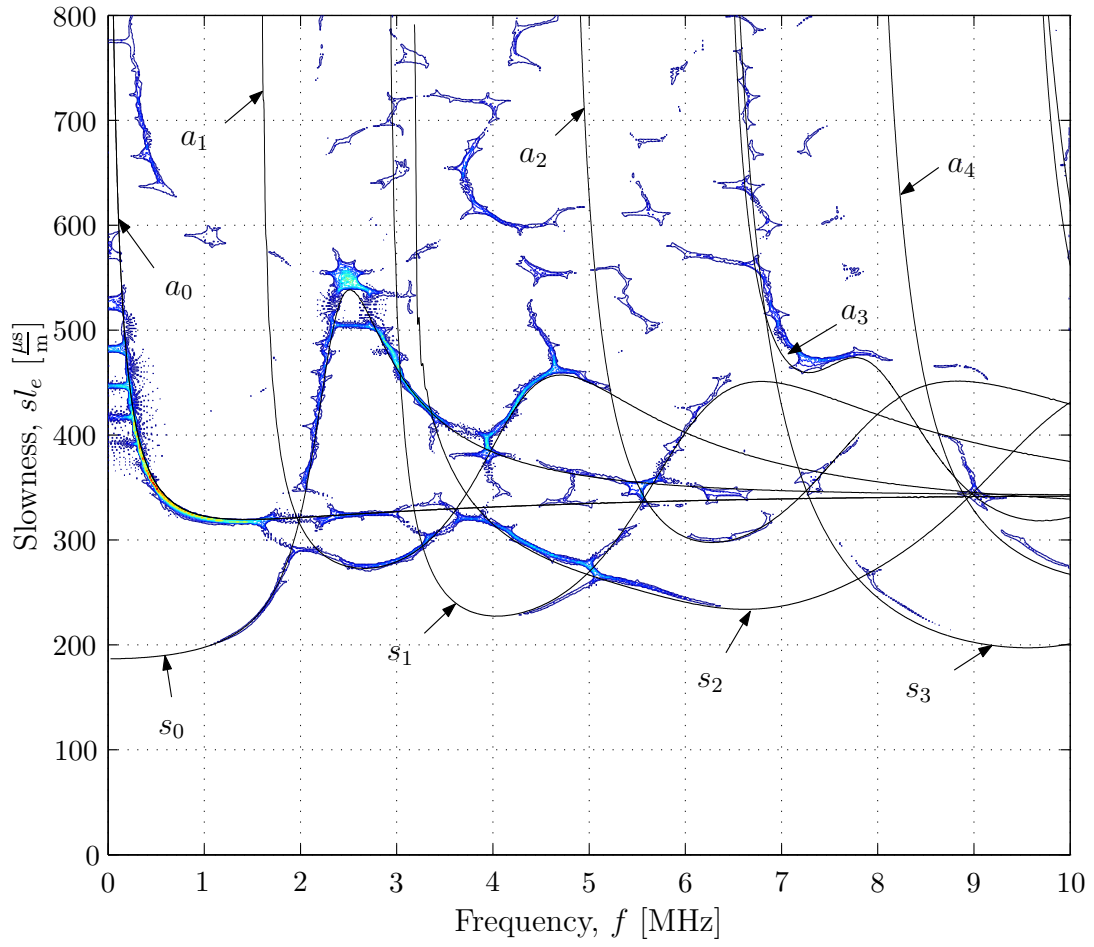


FIG. 3(a). SFR of notched plate, probe 1, source to receiver distance ( $d_1$ ) of 70 mm.

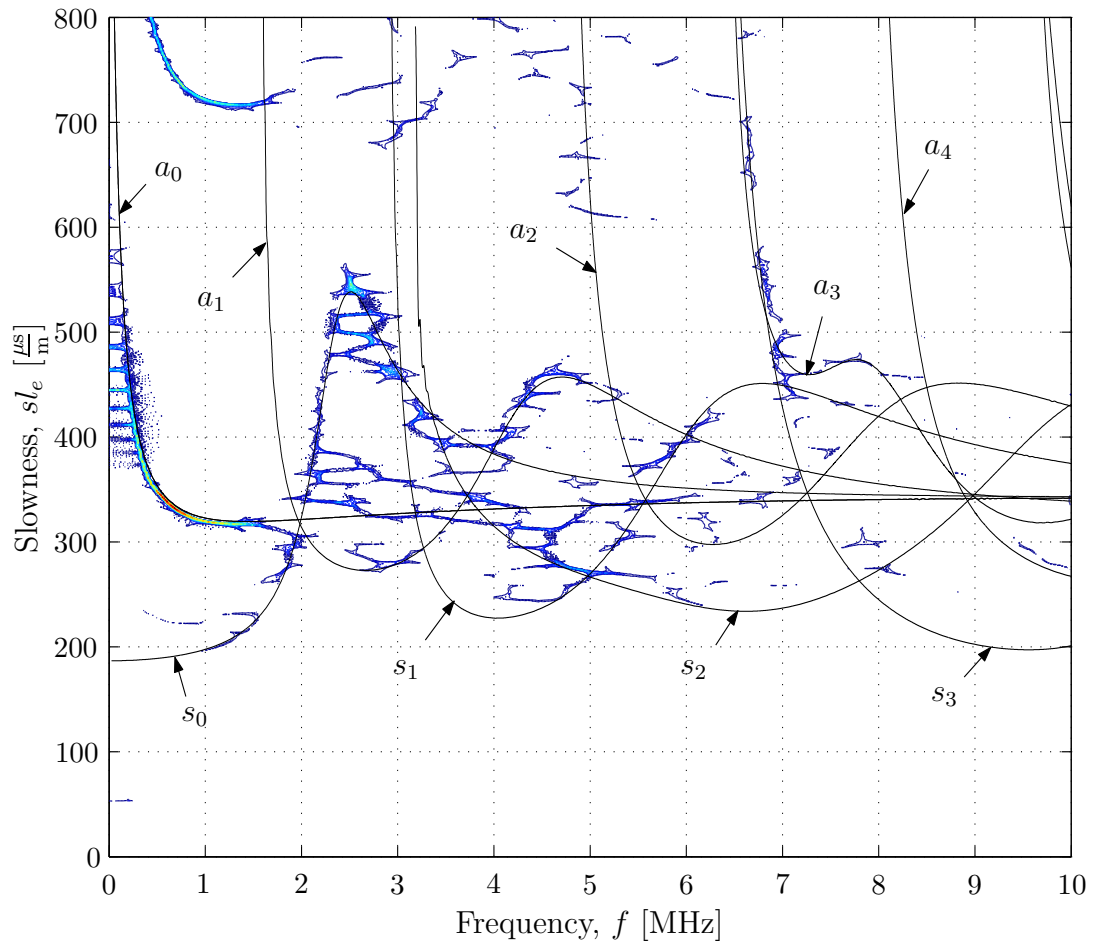


FIG. 3(b). SFR of notched plate, probe 2, source to receiver distance ( $d_4$ ) of 130 mm.

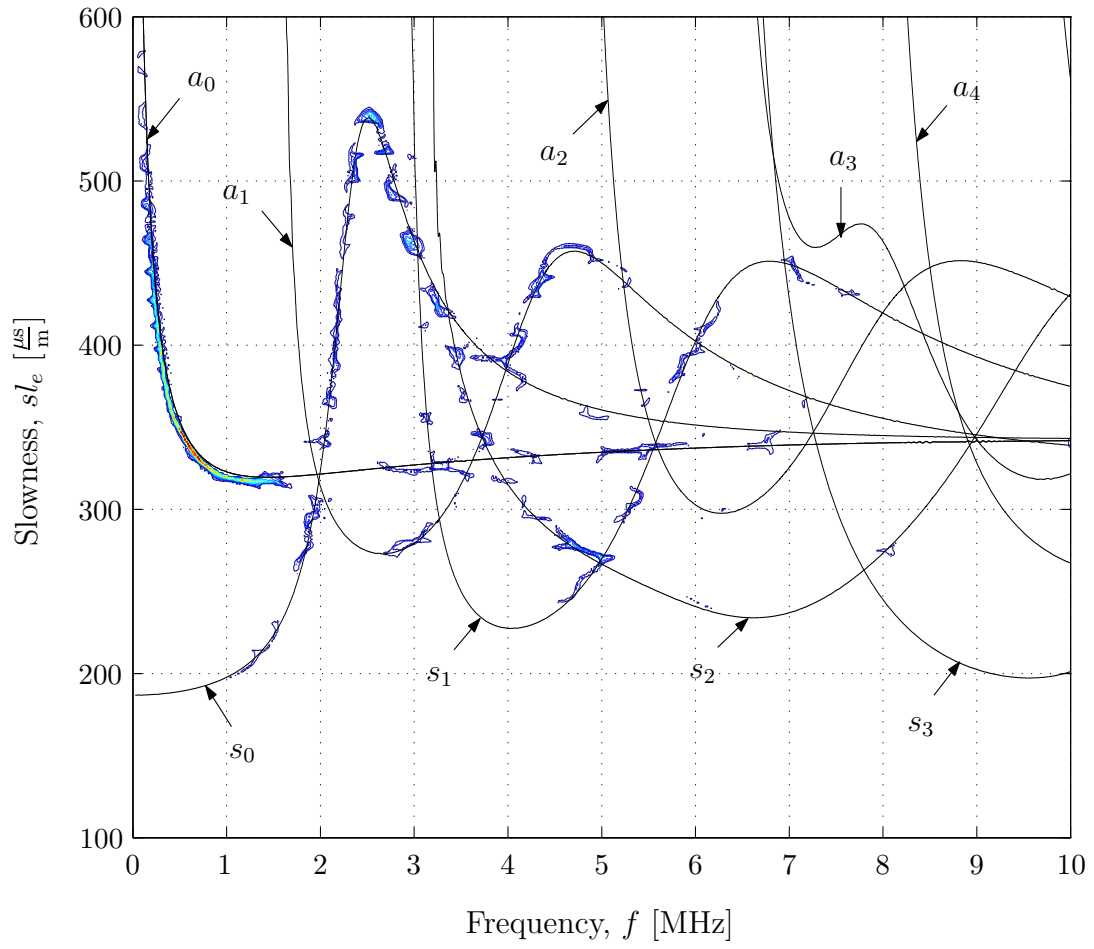


FIG. 4. SFR of modes belonging to case P2b, transmitted and non-mode-converted.

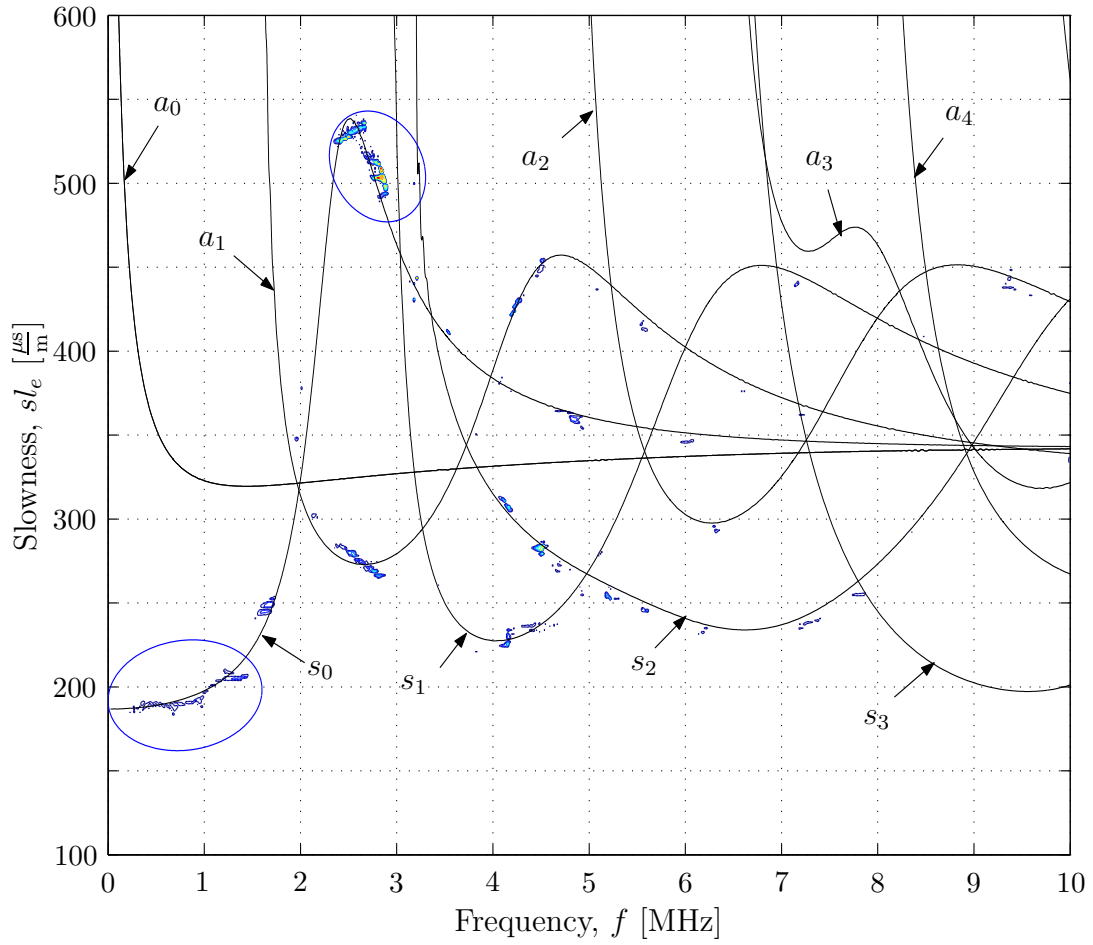


FIG. 5(a). Subset of extraneous modes (transmitted) assuming mode conversion to mode  $a_0$ , new coordinates.

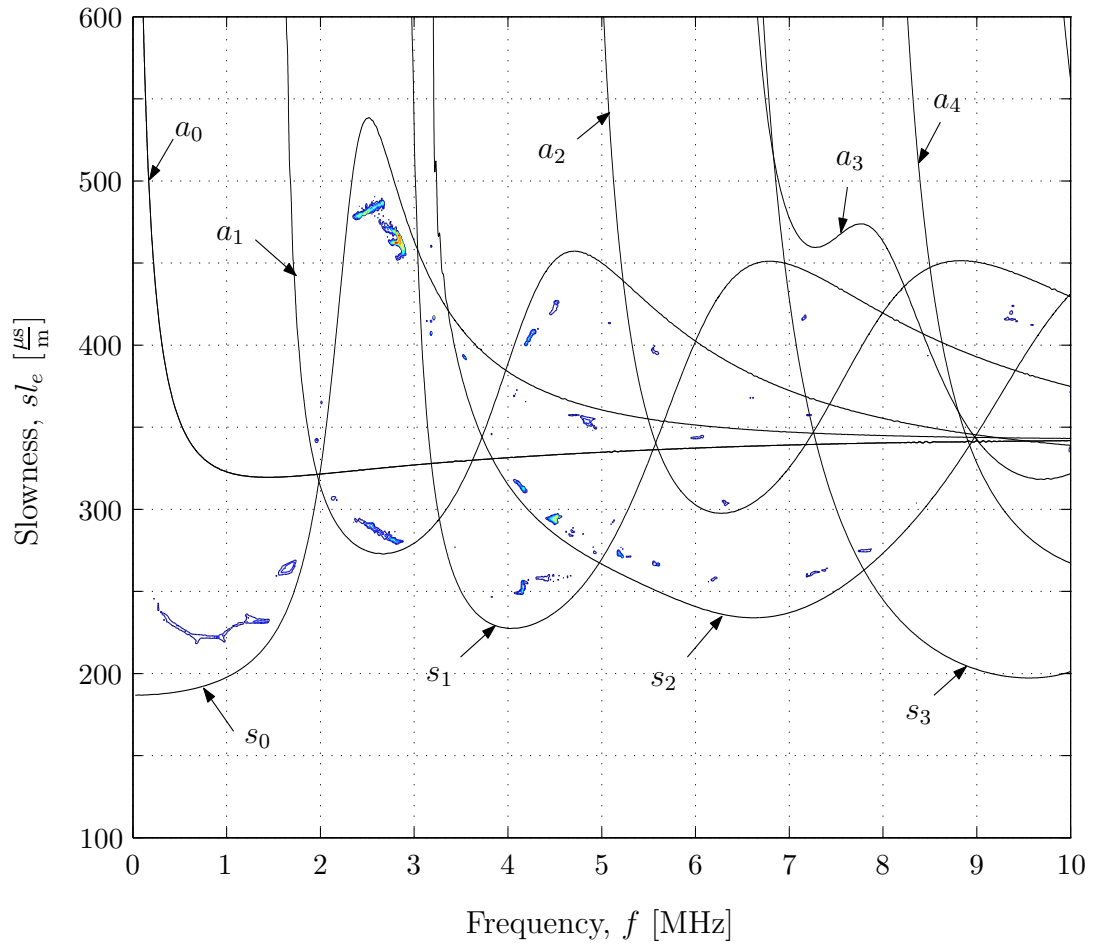


FIG. 5(b). Subset of extraneous modes (transmitted) assuming mode conversion to mode  $a_0$ , original coordinates.

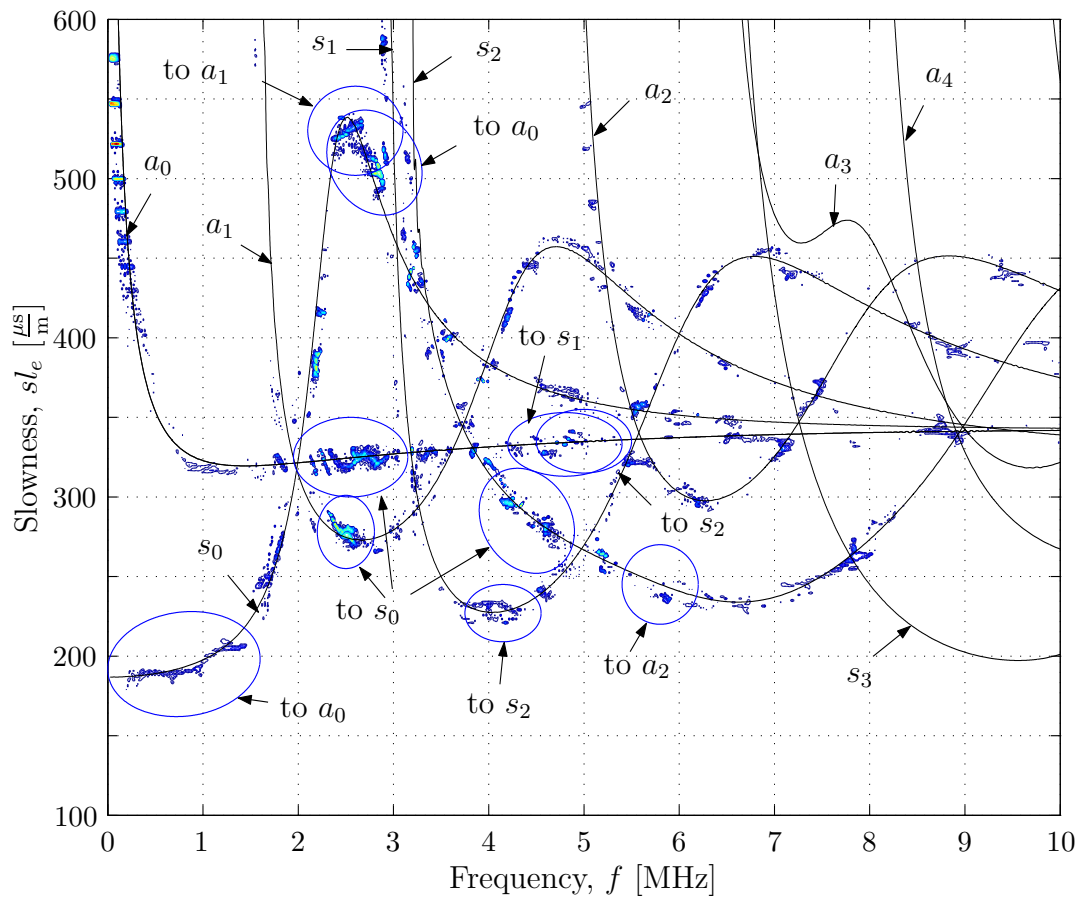


FIG. 6. SFR of modes belonging to case P2c, transmitted and converted.



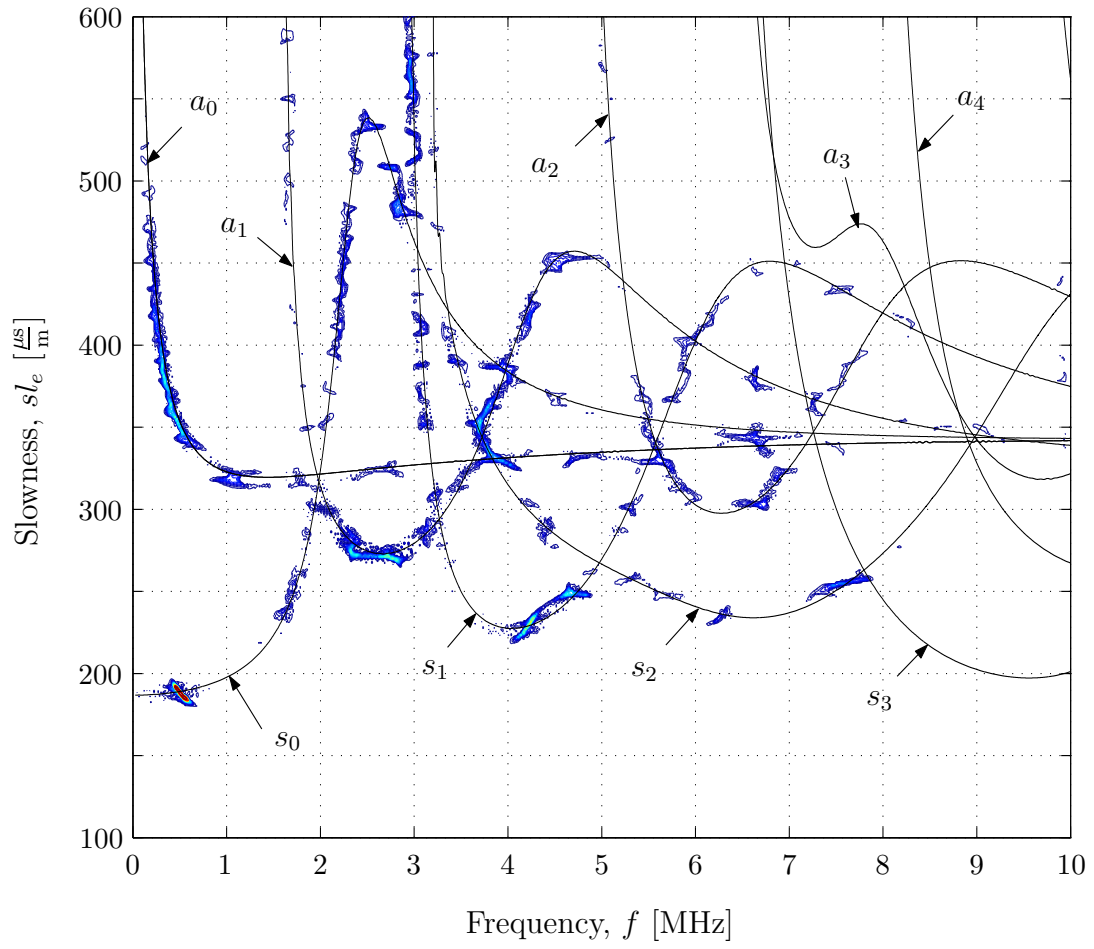


FIG. 7. SFR of modes belonging to case P1b, reflected and non-mode-converted.

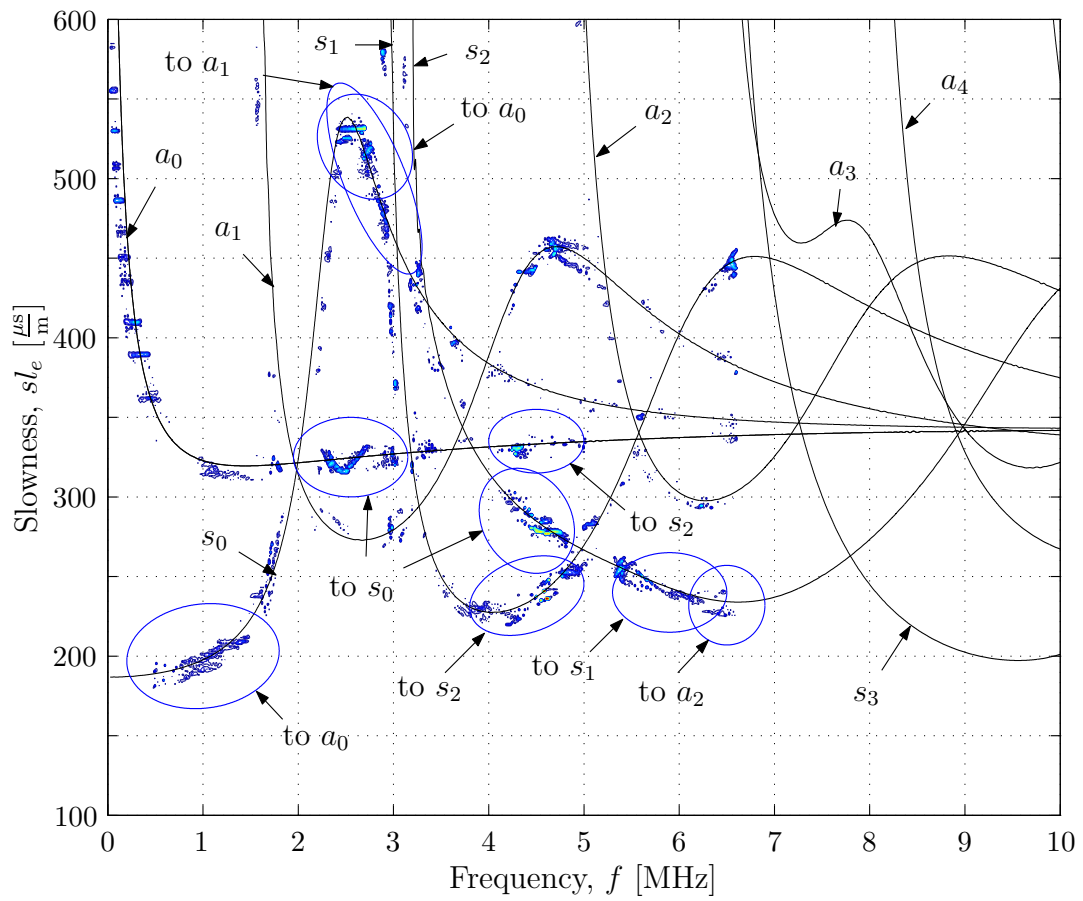


FIG. 8. SFR of modes belonging to case P1c, reflected and converted.

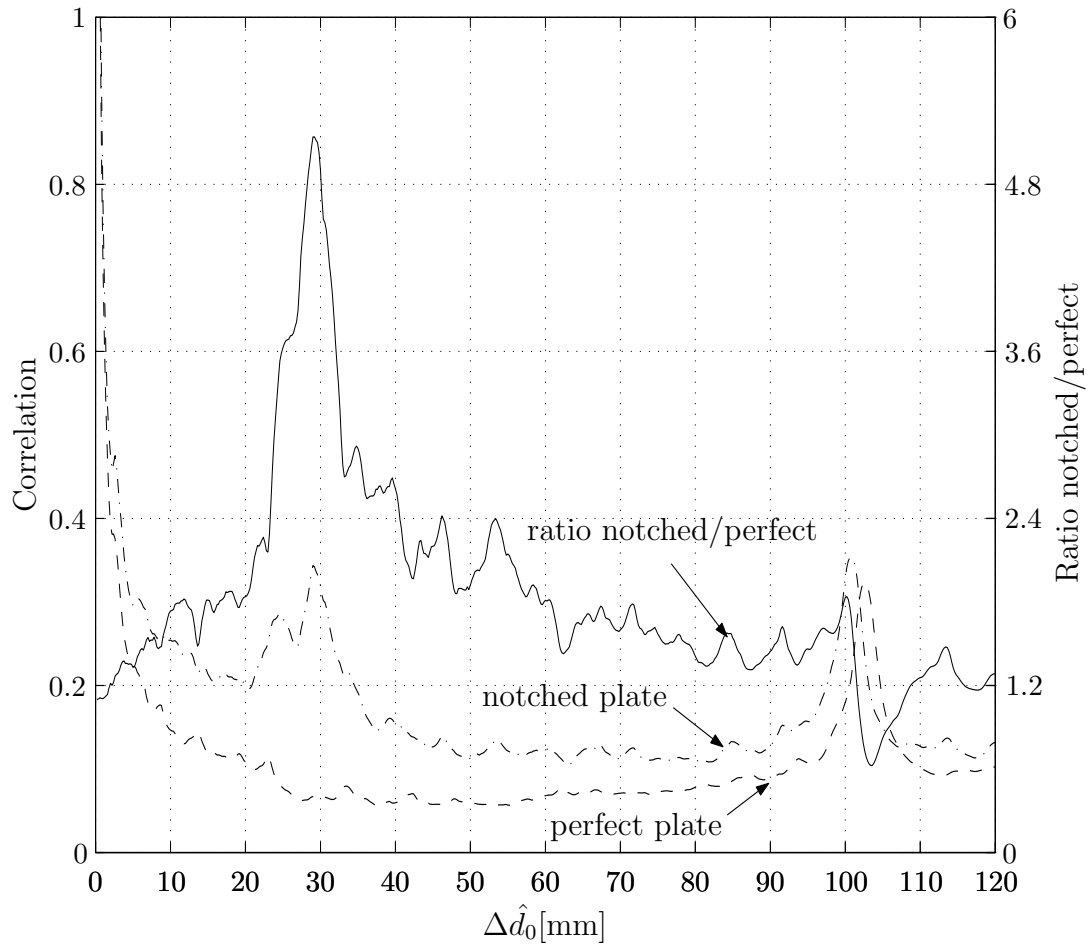


FIG. 9. Correlation curves for the perfect plate, notched plate, and a division of both curves, 0–10 MHz frequency bandwidth, reflected contribution.

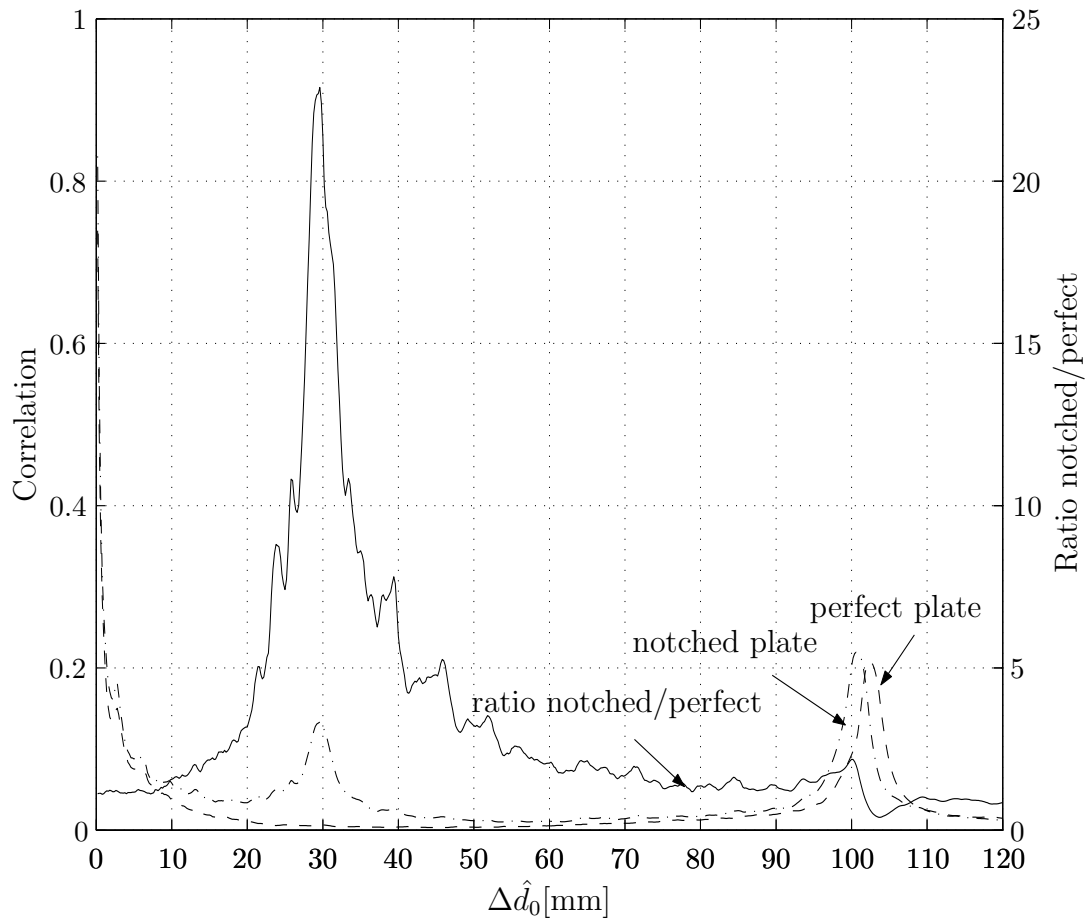


FIG. 10. Correlation curves for the perfect plate, notched plate, and a division of both curves, 0–2 MHz, frequency bandwidth, reflected contribution.

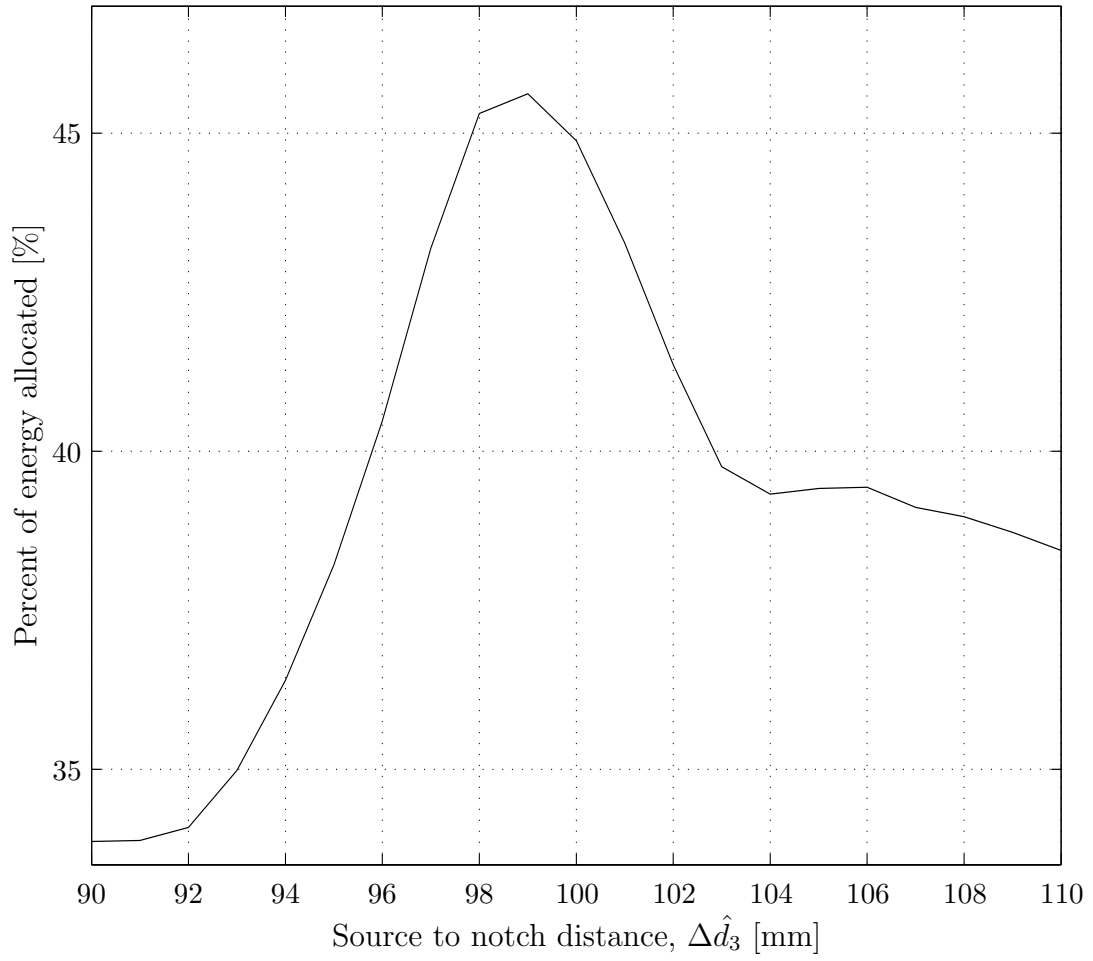


FIG. 11. Goodness-of-fit (as a function of percent allocated) of the allocation of extraneous modes to case B2, used to locate the notch with transmitted contribution.